

MAPPING SEAGRASS PERCENT COVER AND BIOMASS IN NUSA LEMBONGAN, BALI, INDONESIA

Devica Natalia Br Ginting¹, Pramaditya Wicaksono^{1*}, Nur Mohammad Farda¹

¹Faculty of Geography, Gadjah Mada University, Yogyakarta, 55281, Indonesia

*Corresponding author: prama.wicaksono@ugm.ac.id

Received: May 11th, 2023 / Accepted: February 7th, 2024 / Published: March 31st, 2024

<https://DOI-10.24057/2071-9388-2023-2886>

ABSTRACT. Seagrass meadow is one of the blue-carbon ecosystems capable of absorbing and storing carbon more effectively in the bodies and sediments than terrestrial ecosystems. However, nationwide data on its carbon stock remains elusive due to limitations and challenges in data collection and mapping. Seagrass percent cover and biomass, which were closely related with above-ground carbon stock, can be effectively mapped and monitored using remote sensing techniques. Therefore, this study aimed to compare the accuracy of 4 scenarios as well as assess the performance of random forest and stepwise regression methods, for mapping seagrass percent cover and biomass in Nusa Lembongan, Bali, Indonesia. The scenarios were experimented using only atmospherically corrected images, sunglint, water, as well as sunglint and water column corrected images. Furthermore, WorldView-3 images and in-situ seagrass data were used, with the image corrected by applying the scenarios. Random forest and stepwise regression methods were adopted for mapping and modelling. The optimum mapping scenario and method were chosen based on R^2 , RMSE, and seagrass spatial distribution. The results show that the atmospherically corrected image produced the best seagrass percent cover and biomass map. Range of R^2 using random forest and stepwise regression model was 0.49–0.64 and 0.50–0.58, with RMSE ranging from 18.50% to 21.41% and 19.36% to 20.72%, respectively. Based on R^2 , RMSE, and seagrass spatial distribution, it was concluded that the random forest model produced better mapping results, specifically for areas with high seagrass percent cover.

KEYWORDS: WorldView-3, Percent cover, Biomass, Random forest, Stepwise

CITATION: D. N. Br Ginting, P. Wicaksono, N. M. Farda (2024). Mapping Seagrass Percent Cover And Biomass In Nusa Lembongan, Bali, Indonesia. *Geography, Environment, Sustainability*, 1(17), 16-27
<https://DOI-10.24057/2071-9388-2023-2886>

ACKNOWLEDGEMENTS: The authors are grateful to Ignatius Salivian Wisnu Kumara for providing the insitu data. The authors are also thankful to the National Research and Innovation Agency and the Program “Rekognisi Tugas Akhir” (RTA) UGM 2022, for supporting and facilitating this study.

Conflict of interests: The authors reported no potential conflict of interest.

INTRODUCTION

Seagrass is an ecosystem with numerous benefits, including protection services, serving as primary producers, providing habitats for marine biota, and carbon storage (Duarte and Tomas 2013; Macreadie et al. 2017; Sjafrie et al. 2018; Macreadie et al. 2019; Duarte et al. 2020). Compared to terrestrial vegetation, it can store more CO₂ in the bodies and sediments (McLeod et al. 2011). Despite these benefits, seagrass is experiencing a decline of 2-5% annually on a global scale (Duarte and Dennison, 2008). This ecosystem is vulnerable to damage and degradation due to increased coastal development and activities (Grech et al. 2012; Yaakub et al. 2014; Holon et al. 2015), as well as changes in environmental conditions that lead to the extinction of certain species (Strydom et al. 2017). According to study conducted by P2O-LIPI through the COREMAP-CTI project between 2015 – 2017, seagrass beds in Indonesia were in poor condition (Sjafrie et al. 2018). Given this situation, the significance of the mapping and obtaining up-to-date information on the extent and condition of seagrass is increasing (UNEP, 2020).

Remote sensing technology is an efficient and effective tool for monitoring seagrass beds due to its ability to provide both spatial and temporal information (Koedsin et al. 2016; Fauzan et al. 2017; Effrosynidis et al. 2018). Various method can be used to analyze remote sensing data (Effrosynidis et al. 2018; Pham et al. 2019), enabling the provision of information on seagrass extent and changes, species distribution, percent cover (Roelfsema et al. 2014; Fauzan et al. 2021), and biomass (Lyons et al. 2015; Koedsin et al. 2016; Wicaksono et al. 2021).

Seagrass mapping using remote sensing comprises various processes, contributing to producing accurate maps, such as atmospheric, sunglint, and water column correction, as stated in previous studies (Bukata et al. 1995; Hedley et al. 2005). While some investigations suggested that correction can improve accuracy (Tamondong et al. 2013; Anggoro et al. 2016), others indicated the opposite (Zhang et al. 2013). In addition to correction-related reports, data analysis is another critical process in remote sensing, facilitating data interpretation and visualization (Lillesand et al. 2015). The commonly used approach is stepwise regression method, as it enables the selection of an independent variable based on a significant relationship

(Thompson 1995; Smith 2018). This approach accelerates the selection and analysis of the most influential independent variables (Wang and Jain 2003; Khogkhao et al. 2017; Wicaksono et al. 2021). The application of linear regression is challenging due to the complexity of seagrass with diverse habitats and varying density. Alternatively, random forest regression method is a machine learning approach that builds decision trees based on random vectors with independently sampled data. It can unveil more complex relationships and process data quickly and accurately (Salford Systems, 2014; Genauer and Poggi, 2020; Zhang and Xie, 2012; Zhang et al., 2013; Effrosynidis et al., 2018; Maxwell et al., 2018; UNEP 2020).

The study specifically focuses on percent cover and biomass mapping, with previous investigation presenting these parameters as crucial indicators for estimating carbon stocks in seagrass beds (Wahyudi et al., 2019). Remote sensing techniques have been adopted for the mapping process, as showed by Roelfsema et al. (2014), Koedsin et al. (2016), Fauzan et al. (2021), and Wicaksono et al. (2021). Given the importance of seagrass beds in mitigating climate change by sequestering carbon, there is a growing need for data and knowledge on these variables (Duarte and Tomas, 2013; Fourqurean et al., 2013). Therefore, using remote sensing technology to obtain information on percent cover and biomass is crucial. This study aimed to examine various correction methods and compare the effectiveness of the random forest and stepwise regression methods for mapping percent cover and seagrass biomass in Nusa Lembongan Island.

MATERIALS AND METHODS

Study Area

Nusa Lembongan, an island in the Klungkung Regency, Bali, Indonesia (Fig. 1), is geographically located at $08^{\circ} 30' 40''$ - $08^{\circ} 41' 43''$ S, and $115^{\circ} 25' 36''$ E - $115^{\circ} 28' 20''$ E. The

island has a flat topography with northward and southward slopes of 0–3% and 3–8%, respectively. The study area had a coastline of 16.3 km and comprised of mud, rock, and mangrove (Kumara 2018). Nusa Lembongan has a semi-diurnal tide pattern, resulting in two high and two low tides in a day. The current patterns in its waters were influenced by the movement of water masses from the Bali Strait, Lombok Strait, and the Indonesian sea, while tides have a more significant impact on current types in shallow waters (Prasetya et al., 2017).

According to field observations made by the Coral Triangle Center and Udayana University, the Nusa Penida Marine Protected Area has an area of 108 hectares covered by eight species of seagrass, namely *Thalassia hemprichii*, *Halophila decipiens*, *Halophila ovalis*, *Enhalus acoroides*, *Cymodocea rotundata*, *Syringodium isoetifolium*, *Cymodocea serrulata*, and *Halodule uninervis* (Kabupaten Klungkung, 2012). The seagrass ecosystem in the study area comprised of sand and muddy sand substrate types (Negara et al., 2020). However, Negara et al. (2020) stated that seagrass beds in the area were mainly used for tourism purposes, with the majority of the seagrass region serving as docking points for ships.

Field Data

The field data used in this study was sourced from Kumara (2018), who conducted a survey on benthic habitat and seagrass percent cover on Nusa Lembongan Island from June 12 to 19, 2017. This dataset comprised information related to various benthic types, such as coral, seagrass, macroalgae, and bare substrate, with data points distribution of 155, 450, 17, and 194, respectively.

The photo-transect method, which adopted underwater cameras and quadrants, was applied to collect the seagrass percent cover data. The photos taken contained coordinate information as the camera time is synchronized with GNSS. Furthermore, the receiver tracking interval is one second,

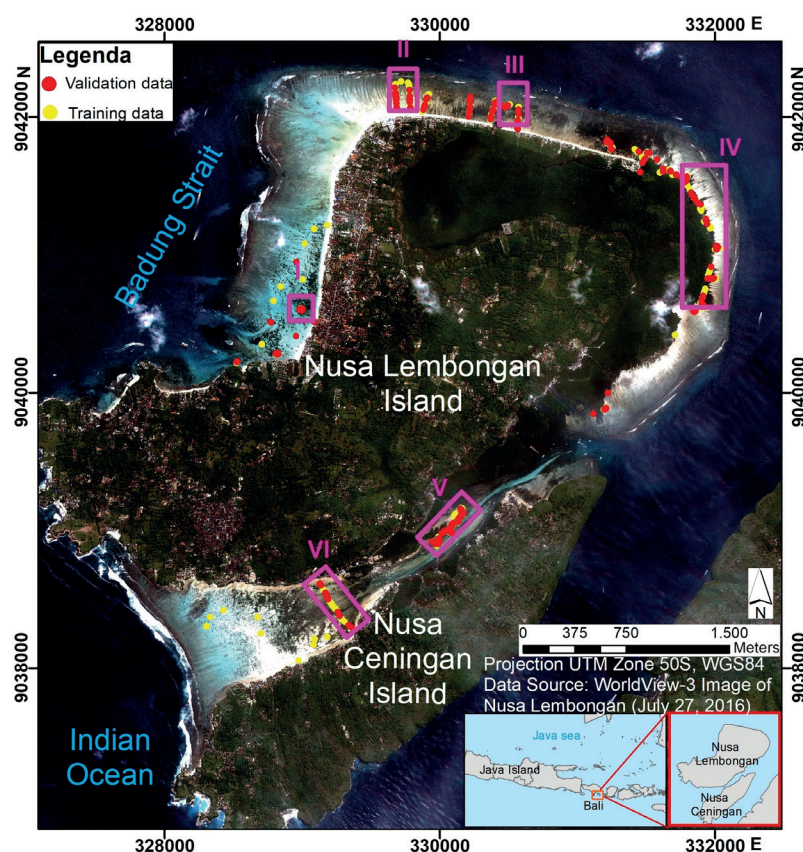


Fig. 1. The study site on Nusa Lembongan Island, as captured by WorldView-3 image. The purple rectangles on the figure represent the various coastal typology zones, while the points indicate the locations of the sample sites

ensuring precise geotagging. Quadrants measuring 0.5×0.5 m were used, and photos were captured at 2 m intervals. These quadrants served as a tool for scaling objects in photos or determining the percentage of seagrass cover. The classification of seagrass percent cover was established according to Fig. 2. For example, when the seagrass covers the entire area of the quadrat, it is labelled as 100%.

Each transect, ranging from 100-150 m long, was divided according to the coastal typology zones, comprising Zone I to VI, namely deep rocky, deep sandy, sandy sloping, muddy sloping, strait sloping, and sandy zones with high currents, respectively. This partitioning facilitated the identification of areas where specific seagrass species were predominantly discovered in each zone. The percent cover on each zone is presented in Table 1. Each zone consisted of 4-6 transect lines, determined by the level of species diversity observed. The field data was divided into two sets. One and one part was used to train the classification and regression models, while the other set was reserved for accuracy assessment.

WorldView-3 Image

DigitalGlobe launched WorldView-3 in 2014 as a commercial high-resolution image. It captures 8 multispectral bands with a spatial resolution of 1.24 m and 8 short infrared bands at 3.7 m resolution, alongside 12 Cavis bands at 30 m resolution, as presented in Table 2. The panchromatic band has a resolution of 0.31 m, and according to Kovacs et al. (2018), high spatial resolution imagery offers increased detail and is commonly regarded as more representative for mapping purposes. This image can capture up to 680,000 km² per day and has been corrected for sensor distortion. The received pixels were in radiometrically calibrated digital number (DigitalGlobe, 2014). The Worldview-3 image used in this study was captured on July 27, 2016, at 10:00:00 AM, when the waters in Nusa Lembongan Island were in low tide. As a result, several benthic objects were visible above the surface at the time of capture. This study used only the visible and near-infrared bands.

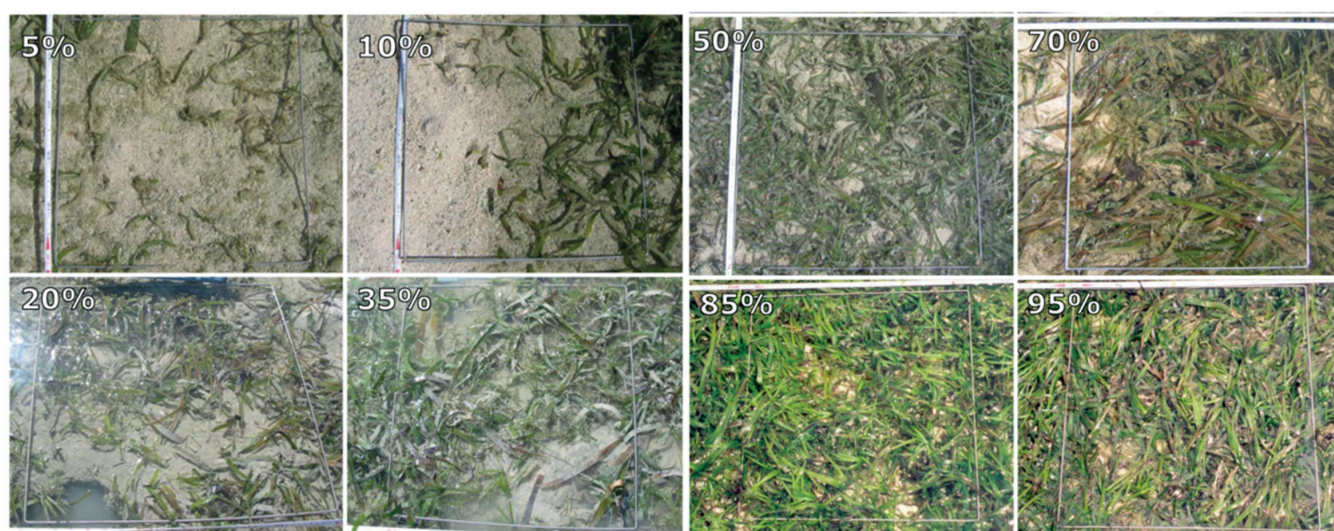


Fig. 2. Seagrass percent cover interpretation guide (seagrasswatch.org, accessed April 10, 2022)

Table 1. Seagrass percent cover on each zone

Zone	Total number of field data	Average (%)
1	49	74.59
2	65	26.17
3	36	47.92
4	84	73.57
5	180	51.75
6	22	55.45

Table 2. WorldView-3 specification

Band	Wavelength (nm)	Band	Wavelength (nm)
Coastal	400 - 450	Red	630 - 690
Blue	450 - 510	Red edge	705 - 745
Green	510 - 580	Near-IR1	770 - 895
Yellow	585 - 625	Near-IR2	860 - 1040
Spatial resolution	1.24 m		
Radiometric resolution	11-bit		
Temporal resolution	Daily		

Image Processing

The initial phase of image processing comprises masking, followed by correction using Scenario 1 - atmospheric, Scenario 2 - sunglint, Scenario 3 - water column, as well as Scenario 4 - sunglint and water column corrections. The corrected image is then used to create maps of benthic habitat and percent cover. Furthermore, the benthic habitat was characterized based on random forest classification algorithm. Pixel values within the seagrass and substrate classes were analyzed using both random forest and stepwise regression methods to produce percent cover map. This percent cover was further transformed into biomass map through the application of equation developed by Wicaksono (2015). The flowchart showing the methodology of this study is presented in Fig. 3.

Image Masking

The process of image masking was adopted to eliminate unnecessary pixels. This includes masking out land, optically deep water, and wave breaking pixels. To achieve land masking, the threshold value of the NIR band was used, enabling the differentiation of water and land pixels. Similarly, water column-corrected bands were used to identify threshold values for deep water pixels, thereby masking out optically deep waters (Wicaksono et al. 2021).

Atmospheric Correction

Atmospheric correction was conducted to obtain the surface reflectance values. The method for removing path radiance in images is the dark object subtraction (DOS) technique developed by Chavez (1996), which is applied to the TOA reflectance of the WorldView-3 image (Equation 1).

$$\rho_{BOA} = \rho_{TOA} - \rho_e \quad (1)$$

where:

ρ_{BOA} : surface reflectance,

ρ_e : reflectance of dark object,

ρ_{TOA} : reflectance on top of atmosphere

Sunglint Correction

In this study, the method developed by Hedley et al. (2005), was applied to reduce sunglint by leveraging the linear relationship between the NIR and visible bands in a training area with various sunglint levels. The required inputs for this correction include the visible band to be corrected, the slope of the linear regression, the NIR band, and the minimum value of the NIR band in an area unaffected by sunglint, as shown in Equation 2. The correction process engaged 968 samples obtained from affected deep-water areas. The slope of the linear regression was obtained from a training area of pixels in deep waters with varying sunglint intensities, as determined by Hochberg et al. (2003). The minimum value of the NIR band in the region

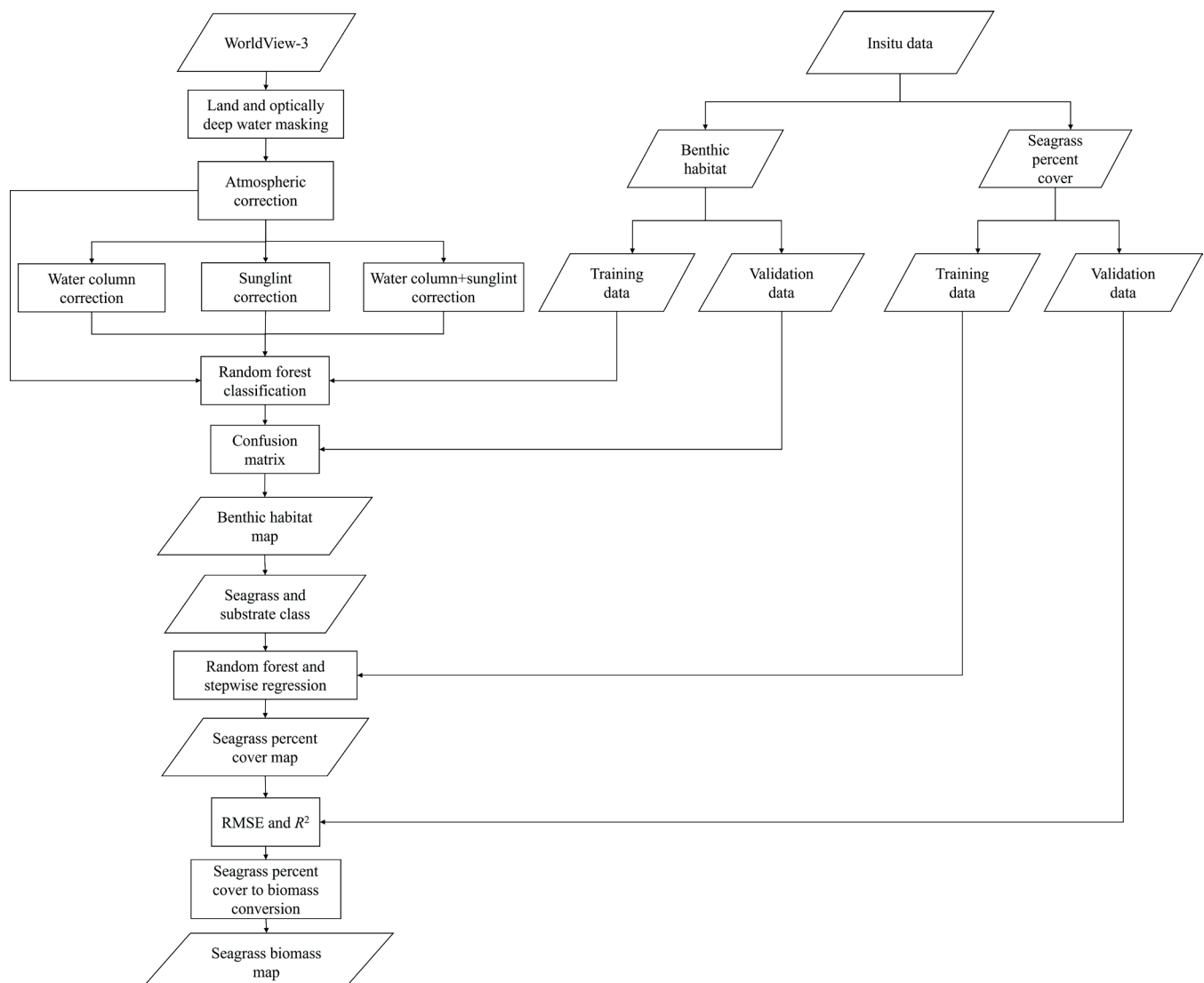


Fig. 3. The study flowchart

without sunglint was calculated by applying the following equation.

$$\rho'_i = \rho_i - b_i(\rho_{NIR} - \rho_{Min_{NIR}}) \quad (2)$$

where:

- ρ_i = reflectance of visible band i
- b_i = slope between visible and NIR
- ρ_{NIR} = reflectance of band NIR
- $\rho_{Min_{NIR}}$ = minimum reflectance of NIR band
- ρ'_i = reflectance of sunglint corrected band

Water Column Correction

This study used the water column correction method developed by Lyzenga (1978), as described in Green et al. (2000). The method adopted a pair of visible bands to generate a new band where the energy attenuation effect from the water column has been minimised. To perform the necessary corrections, reflectance values of the same benthic object at different depths were required (Equation 3). Meanwhile, sand was chosen for this study, as it is easily visible and distinguishable at different depths, with the reflectance value decreasing as depth increases. A total of 217 samples of sand were collected at various depths.

$$Y = \ln(L_i) - \left[\left(\frac{k_i}{k_j} \right) \ln(L_j) \right] \quad (3)$$

where:

- Y = depth invariant index
- L_i = reflectance of band i
- L_j = reflectance of band j
- k_i/k_j = ratio of coefficient attenuation for band i dan j

Mapping Methods

Random Forest

Random forest is a machine learning approach that builds decision trees based on random vectors with independently sampled data (Salford Systems, 2014; Genuer and Poggi, 2020). Its classification and regression was used for benthic habitat and seagrass percent cover mappings, respectively. In random forest regression, n_{tree} (the number of trees) and m_{try} (the number of variables randomly selected at each node) parameters were also set. Furthermore, n_{tree} used factors of 100 and 500, while for m_{try} , the total of input variables was divided by 3 (Genuer and Poggi, 2020) and the lowest error from out-of-bag (OOB). The first m_{try} was the initial m_{try} in R software, and second mtry OOB was chosen because OOB samples help evaluate misclassification as well as estimate the importance of variables (Eisavi et al., 2015).

Stepwise Regression

Stepwise regression is an analysis method used to determine the relationship between independent and dependent variables. This was achieved analysing the sequence of significant relationships among the independent variables (Thompson, 1995; Smith, 2018). In this study, stepwise regression was used to determine the relationship between reflectance value of the image and the in-situ data on the percent cover. The equation obtained from this analysis was then adopted to generate a spatial distribution of the percent cover on the WorldView-3 image.

Seagrass Biomass

The seagrass biomass map was derived through the conversion of percent cover using the equation provided by Wicaksono (2015). A regression analysis was conducted on in-situ data, establishing a relationship between percent cover and biomass with an R^2 value of 0.4399 and a standard error (SE) ranging from 30 to 40 g/m², as shown in Equation 4. Seagrass PC was the most efficient method for estimating biomass due to its quick and non-destructive nature (Wicaksono, 2015). The following represent the equation adopted.

$$AGB_{seagrass} = 1.2712(PCy) + 6.6016 \quad (4)$$

With PCv is seagrass percent cover

Accuracy Assessment

Benthic habitat mapping accuracy assessment was performed using the confusion matrix method. This approach adopted a table that evaluates the classification algorithm performance (Ting, 2017). The overall accuracy was determined by calculating the number of pixels accurately classified against the field data. In testing empirical modelling for percent cover and biomass, the coefficient of determination (R^2) and root mean square error (RMSE) were used. The R^2 measures the goodness-of-fit of the model to the data (Ozer, 1985). On the other hand, the RMSE is a statistical method that assesses the model accuracy (Chai and Draxler, 2014). The error value represented the difference between the model results and the in-situ data. This assessment is essential in evaluating the accuracy of each scenario and the results obtained was compared using the random forest and stepwise regression methods.

RESULTS

Benthic habitat Mapping

Benthic habitat maps were generated using random forest classification in atmospheric scenario, which showed the highest accuracy and spatial distribution in Nusa Lembongan Island (Ginting et al., 2023). The classification outcomes showed the ability to map fringing reef formations, despite the misclassification of seagrass as coral, as indicated by the red circle in Fig. 4.

In atmospheric scenario, the accuracy was 73.00%, while for coral, seagrass, substrate, and macroalgae, the user's accuracies were 83.33%, 71.94%, 69.84%, and 0%, respectively. The corresponding producer's accuracies for the same classes were 56.45%, 87.36%, 57.14%, and 0%. When comparing the user's and producer's accuracies, the results suggest that the reef and substrate classes were underestimated, and the spatial distribution of this ecosystem exceeded estimation. However, due to a lack of field data and the absence of macroalgae in the study area, accurate mapping was not possible.

Seagrass Percent Cover Mapping

The spatial distribution of percent cover in each scenario was analyzed based on the levels specified in the Decree of the Minister of Environment No. 200 of 2004 (Kepmen LH, 2004), which include low (29.9%), medium (30.0–59.9%), and high (> 60%). The analysis was focused on 6 zones, as described in Fig. 1. Seagrass dominated in Zone I and IV, seagrass dominated, showing high percent cover, while Zone II had a low percent cover. Finally, the percent cover in III, V, and VI was moderate.

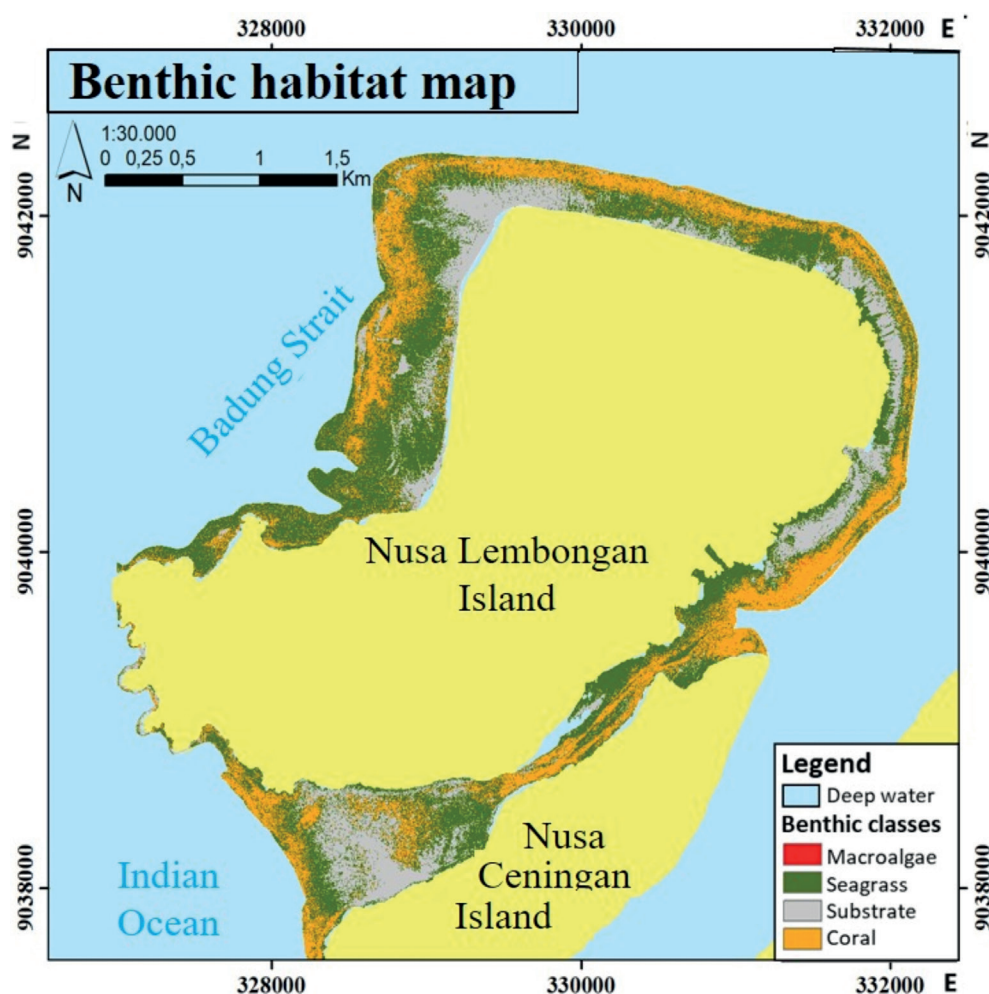


Fig. 4. Benthic habitat map obtained from random forest classification based on atmospheric correction scenario

In random forest regression, parameter tuning is conducted to analyze the effect of each parameter (n_{tree} and m_{try}) on the mapping of percent cover. The R^2 did not show a significant difference between parameter tuning, as indicated by the small variation in its values (0-0.2), as presented in Table 3. Based on RMSE, the error difference between m_{try} ranged from 0.03-0.31%, while n_{tree} was spanned between 0.09-0.76%. The initial m_{try} showed the lowest RMSE among all m_{try} parameter tuning. This study concluded that the n_{tree} parameter had the most influence on the accuracy of the percent cover map, with the lowest RMSE observed at n_{tree} 500. The range of R^2 and RMSE in the 4 scenarios are 0.49-0.64 and 18.50-21.41%, respectively. The ranking of R^2 from highest to lowest include Scenario 2, Scenario 4, Scenario 1, and Scenario 3. On the other

hand, the best RMSE was indicated by the lowest value, observed in Scenario 4, followed by Scenario 2, Scenario 3, and Scenario 1.

In Scenario 1, based on random forest regression, seagrass with medium-to-high percent cover can be mapped as apposed to those with low cover percent, as shown in Fig. 5. On the other hand, Scenario 2 is unable to map high percent cover in coastal areas near mangroves (Zone IV) due to the pixel value loss caused by the sunglint correction process (marked by white on the map). Analyzing the distribution in each zone showed that Scenario 2 adequately maps the percent cover of zones III, V, and VI. However, misclassifications occurs in Zone II, where low percent cover is classified as a medium cover.

Table 3. R^2 and RMSE based on random forest regression

Scenario	n _{tree}							
	100				500			
	R ²	RMSE (%)	R ²	RMSE (%)	R ²	RMSE (%)	R ²	RMSE (%)
1	0.61	21.41	0.61	21.35	0.61	21.07	0.61	21.10
2	0.63	19.50	0.64	19.60	0.63	19.34	0.62	19.41
3	0.51	21.4	0.49	21.22	0.50	21.06	0.51	21.13
4	0.62	19.08	0.62	19.26	0.63	18.81	0.62	18.50
	Initial		OOB		Initial		OOB	
	m _{try}							

Scenario 3 had the lowest R^2 and higher error compared to the others, indicating a higher level of misclassification due to the correction process. Examining the spatial distribution in each zone show that this scenario is effective at mapping the percent cover in Zones I, and IV, which have a high percent cover. Scenario 4 had similar classification with 2, with missing pixel values denoted by white markings resulting from sunglint correction. This scenario was effective at mapping moderate percent cover but is less effective for low percent cover.

Each scenario was compared using 3 metrics, namely R^2 , RMSE, and spatial distribution, to determine the optimal scenario for mapping biomass. Analysis showed that Scenario 1 (Zones I, II, IV, and VI) and Scenario 3 (zones III and IV) had the best performance, with the highest R^2 and lowest error, as detailed in Fig. 6. Specifically, Scenario 1 proved effective for mapping seagrass with a high percent cover, while 2 was more suitable for objects that are often submerged in water and the ecosystem with a medium percent cover. Based on these results, Scenario 1 was the optimal choice for mapping purposes, considering R^2 , RMSE, and spatial distribution.

Based on the stepwise regression in Table 4, Scenario 1, 2, 3, and 4 had R^2 and RMSE values of 0.53 and 20.65%, 0.58 and 19.36%, 0.50 and 20.72%, as well as 0.56 and 20.61%, respectively. These values showed that Scenarios 2, 4, 1, and 3 were ranked from the best to the worst.

Fig. 7 contains a map showing the percent cover obtained through stepwise regression. While Scenario 1 is proficient in mapping from low to high, it misclassifies the percent cover of seagrass. The distribution in zones I, II, IV, V, and VI, was accurately mapped by this scenario, except for zone III dominated by high cover. On the other hand, Scenario 2 maps the percentage of cover in zones I, II, III, V, and VI accurately, except for zone IV due to the loss of seagrass pixel caused by the sunglint correction process. In the mapping process, Scenario 3 also shows the same pattern as Scenario 1. However, certain areas marked as having high percent cover in the Scenario 1 are classified as medium in Scenario 3.

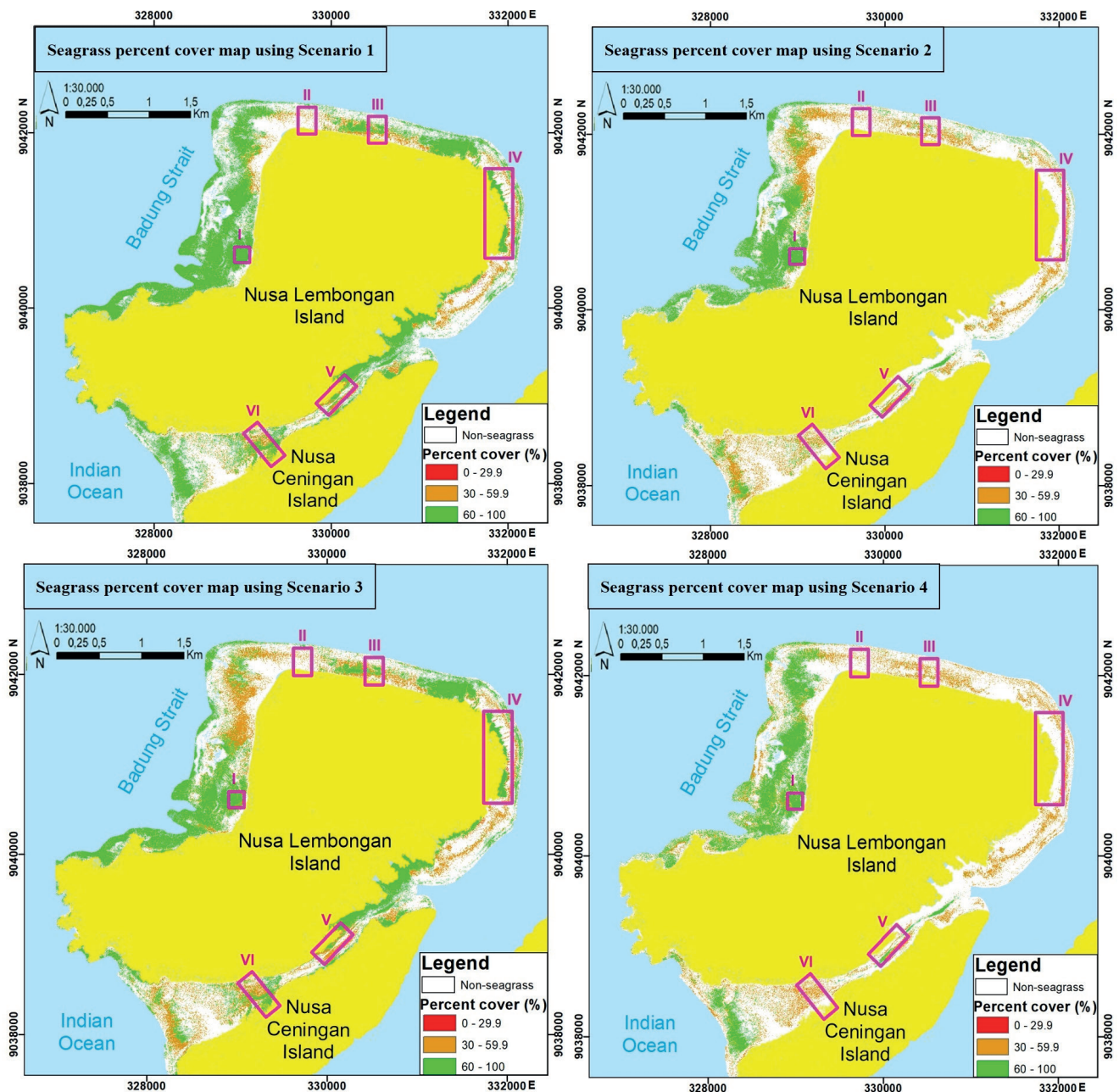


Fig. 5. Seagrass percent cover map based on random forest regression. Red boxes indicate coastal typology zones. The figures illustrate variations in seagrass percent cover based on the four scenarios

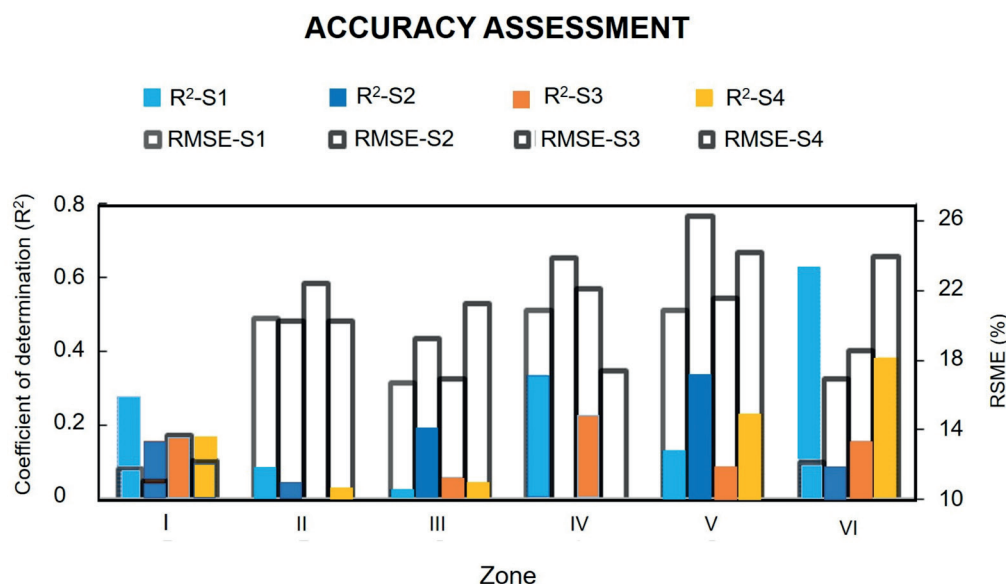


Fig. 6. The accuracy assessment of seagrass percent cover map based on the random forest method for each scenario and zone. The R^2 is represented by the coloured boxes, while the scenarios are distinguished by their respective colours. Boxes with a thick outline indicate the RMSE

Table 4. The R^2 and the RMSE of each scenario

Scenario	R^2	RMSE (%)
1	0.53	20.65
2	0.58	19.36
3	0.50	20.72
4	0.56	20.61

Comparison of seagrass percent cover map using random forest and stepwise regression

Based on the scenario analysis, the random forest regression outperformed the stepwise regression method in terms of the R^2 (Fig. 8) and RMSE values. To compare the spatial distribution of the results obtained from both methods, the scenarios with the highest R^2 and the lowest RMSE were selected. Scenario 1 was chosen for the random forest regression, while Scenario 2 was selected for the stepwise regression. The results showed that the random forest regression provided better spatial distribution of seagrass percent cover. This shows that the method was selected based on its accuracy and spatial distribution of seagrass percent cover.

Seagrass Biomass

In this study, biomass map was obtained by using an equation developed by Wicaksono (2015). This equation demonstrated that mapping seagrass aboveground biomass (g/m^2) can be accomplished by applying information on percent cover. To generate the biomass map, the best value of R^2 , RMSE, and spatial distribution was selected. The accuracy assessment showed that random forest method was most effective for mapping. The results of the biomass map can be viewed in Fig. 9, where high aboveground biomass is located in zones I and IV.

The field data was converted to a percentage of cover for validation using the Wicaksono (2015) equation to assess the accuracy of the aboveground biomass. The atmospheric scenario biomass was compared with that of validation data. Finally, the comparison yielded R^2 and RMSE of 0.38 and 24.33 g/m^2 , respectively.

DISCUSSION

This study aims to examine various correction and compare the effectiveness of the random forest and stepwise regression methods for mapping percent cover and seagrass biomass in Nusa Lembongan Island. Initially, benthic habitats were classified, achieving an accuracy of over 60%, which met the Indonesian National Standard 7716:2011 (BSN 2011). The classification effectively mapped fringing reef formations and seagrass meadow ecosystems in the study area, as shown in the study by Prasetya et al. (2017) and Negara et al. (2020). However, macroalgae objects were not mapped due to the low cover, as presented in the report by Munir and Wicaksono (2019).

Seagrass and sand pixels from benthic habitat were selected to examine various correction and methods to extract seagrass percent cover. Based on the analysis of all data, both the random forest and stepwise regression methods indicate that Scenario 2 had the highest R^2 and the lowest RMSE. However, a closer examination of coastal typology zones shows that the random forest method performs better with Scenario 1, particularly in zones of high seagrass cover. This approach outperforms the stepwise regression method in terms of R^2 and RMSE, both overall and per-zone. Furthermore, an analysis was conducted related to tuning parameters, such as n_{tree} and m_{try} . The random forest method parameter settings indicated that n_{tree} had a more significant effect on RMSE than m_{try} for mapping percent cover. The number of trees is directly proportional to the stability of the model (Dai et al. 2018; Genuer and Poggi 2020).

Scenario 1 was chosen for several reasons. Firstly, the image was captured during low tide, eliminating the

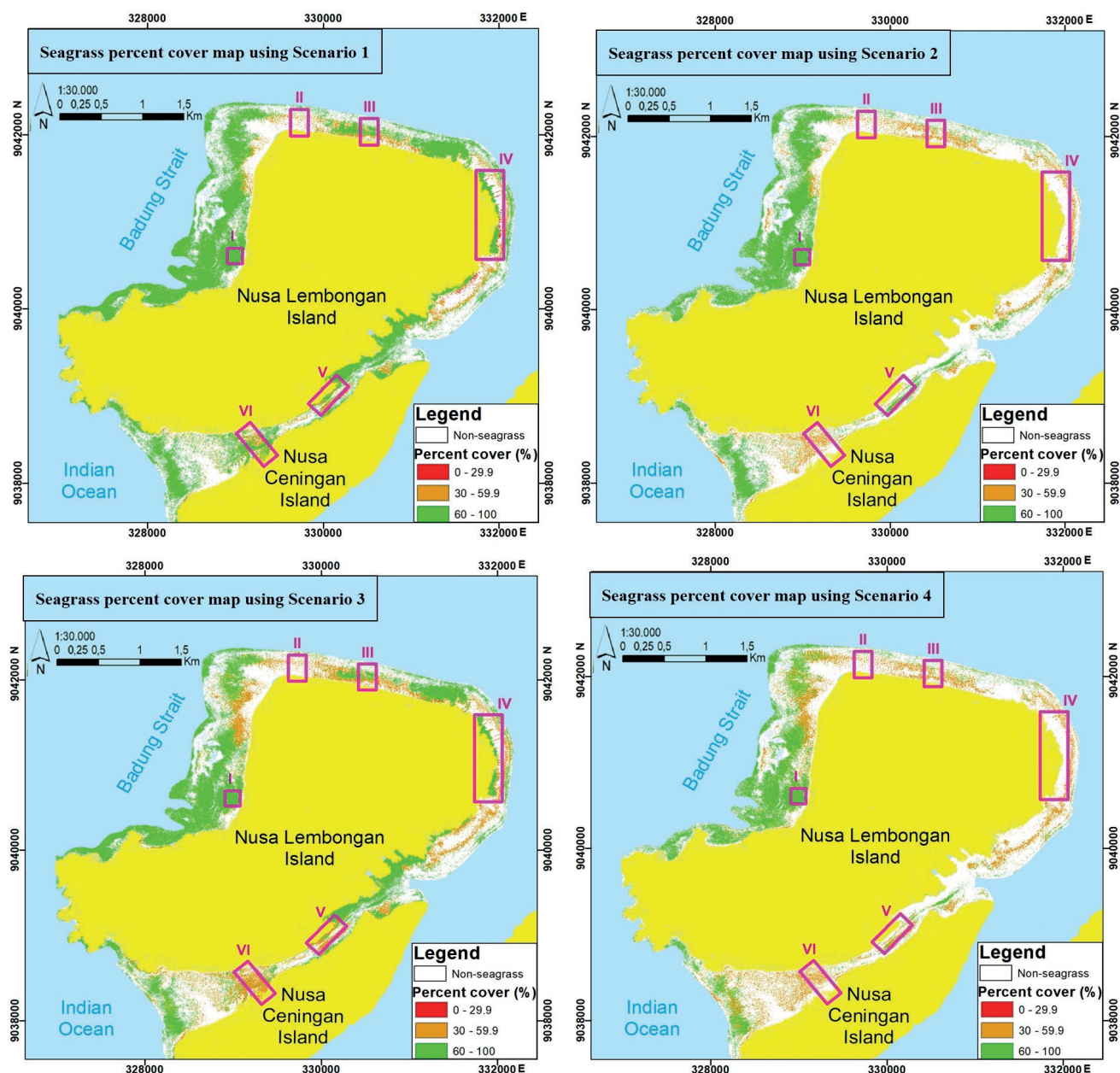


Fig. 7. The map of seagrass percent cover obtained using stepwise regression. Purple boxes indicate the coastal typology zones. The figures display the variation of seagrass percent cover based on four mapping scenarios

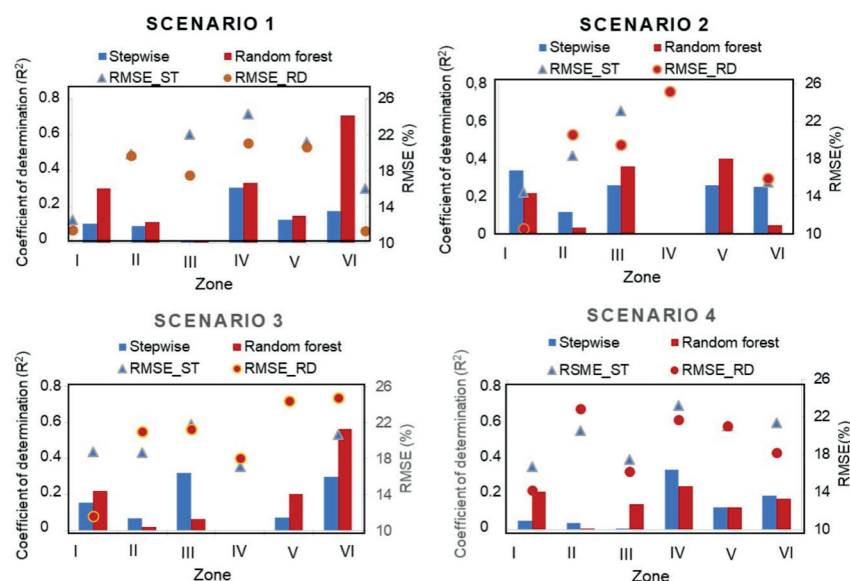


Fig. 8. Comparison of seagrass percent cover map accuracy assessment in each zone for all scenarios, using both random forest and stepwise regression. The rectangles in the figure represent the R^2 , while triangles and circles represent RMSE values

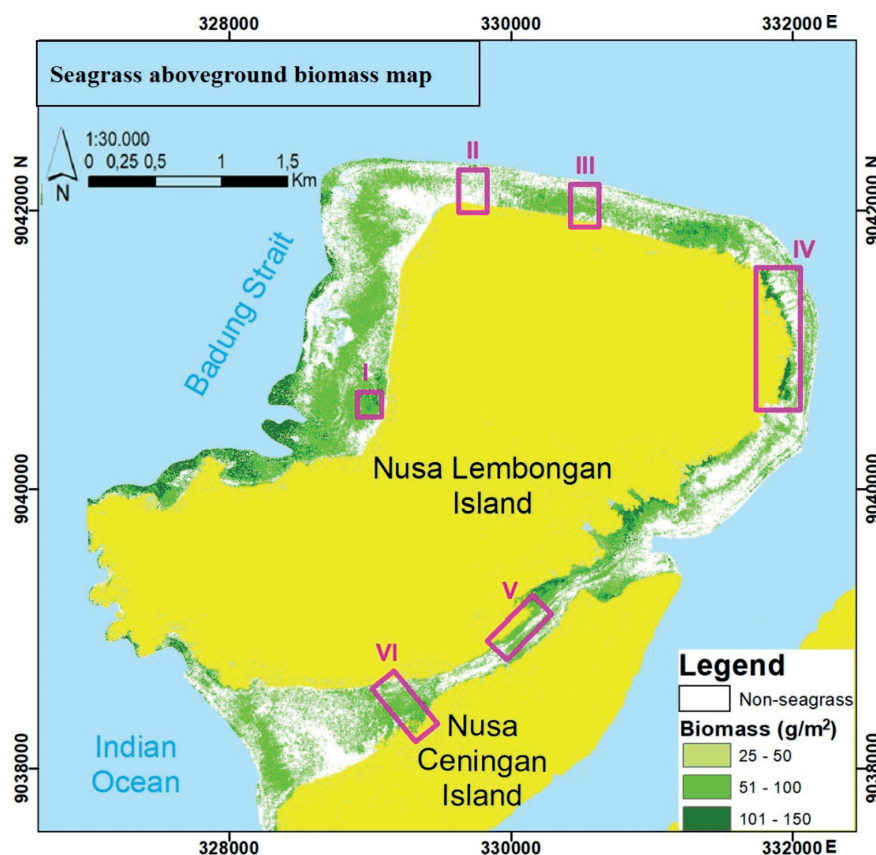


Fig. 9. Seagrass aboveground biomass map

need for water column correction. This was in line with the study of Zoffoli et al. (2014), where it was concluded that the Lyzenga method cannot be used for very shallow waters. Moreover, the images used were recorded at low tide and dominated by field data on reef flats. Secondly, despite sunglint scenario yielding the highest R^2 , it resulted in the loss of pixels above the water surface, particularly seagrasses, after correction. This suggested that atmospheric correction was the best input data for percent cover mapping. Finally, according to Wicaksono et al. (2019), atmospheric correction produced relatively stable values depending on atmospheric conditions.

Compared to the previous investigation on mapping seagrass percent cover, this study indicates better performance than the R^2 generated in Labuan Bajo using Planetscope data and the Support Vector Machine method (Munir et al. 2019). However, the model accuracy was lower than in the study of Ariasari et al. (2019), where Planetscope data and principal component analysis were used on the image to generate input data for random forest regression. Future study should consider the principal component analysis process to improve the accuracy of mapping the percent cover in the study area.

Seagrass percent cover map was adopted to estimate above-ground biomass using the equation from Wicaksono (2015). The result showed that the equation can be used to map above-ground biomass up to 131 g/m². Based on field data collected in 2019 by Negara et al. (2020), the biomass

at the study site ranged from 157.38 to 310.75 g/m², covering 3 zones. This difference in value was due to the equation by Wicaksono (2015) being developed in areas with lower biomass values compared to Nusa Lembongan Island. Despite this, the R^2 results are not significantly different from those of Wicaksono (2015).

The success of WorldView-3 imagery in producing a representative map is attributed to its high spatial and spectral resolution, making it particularly suitable for mapping seagrass ecosystems. These ecosystems are characterized by diverse species, benthic types, and present at varying density. However, WorldView-3 has limitations when applied to large areas or time series analysis. This is primarily due to a lack of scheduled and regular acquisition frequency, thereby making it expensive.

CONCLUSIONS

In conclusion, this study successfully documented the optimal data input for mapping seagrass percent cover based on image and site conditions. The most effective input data for mapping seagrass percent cover using WorldView-3 imagery, recorded at low tide, in a small island and dominated by field data in reef flat areas, was the atmospheric scenario, yielding R^2 and RMSE values of 0.61 and 21.07%, respectively. The random forest algorithm showed superior accuracy compared to the stepwise regression method. ■

REFERENCES

- Anggoro, A., Siregar, V. P., & Agus, S. B. (2016). The Effect of Sunlight on Benthic Habitats Mapping in Pari Island Using Worldview-2 Imagery. *Procedia Environmental Sciences*, 33, 487–495. <https://doi.org/10.1016/j.proenv.2016.03.101>
- Ariasari, A., Hartono, & Wicaksono, P. (2019). Random forest classification and regression for seagrass mapping using PlanetScope image in Labuan Bajo, East Nusa Tenggara. *Proceedings of SPIE - The International Society for Optical Engineering*, 11174, 1117407. <https://doi.org/10.1117/12.2541718>
- Badan Standarisasi Nasional. (2011). SNI 7716/2011: Pemetaan habitat perairan laut dangkal. Jakarta.
- Bukata, R. P., Jerome, J. H., Kondratyev, A. S., & Pozdnyakov, D. V. (1995). *Optical Properties and Remote Sensing of Inland and Coastal Waters*. CRC Press LLC.
- Chai, T., & Draxler, R. R. (2014). Root mean square error (RMSE) or mean absolute error (MAE)? -Arguments against avoiding RMSE in the literature. *Geoscientific Model Development*, 7(3), 1247–1250. <https://doi.org/10.5194/gmd-7-1247-2014>
- Chavez, P. S. (1996). Image-based atmospheric corrections - Revisited and improved. *Photogrammetric Engineering and Remote Sensing*, 62(9), 1025–1036.
- Dai, B., Gu, C., Zhao, E., & Qin, X. (2018). Statistical model optimized random forest regression model for concrete dam deformation monitoring. *Structural Control and Health Monitoring*, 25(6), 1–15. <https://doi.org/10.1002/stc.2170>
- DigitalGlobe. (2014). World View-3 Design and Specifications. www.Digitalglobe.Com, 1–2.
- Duarte, C. M., Dennison, W. C., Orth, R. J. W., & Carruthers, T. J. B. (2008). The Charisma of Coastal Ecosystems: Addressing the Imbalance. *Estuaries and Coasts: J CERF* (2008) 31:233–238. DOI 10.1007/S12237-008-9038-7.
- Duarte, C. M., Tomas, S., & Nuria, M. (2013). Assessing the CO2 capture potential of seagrass restoration projects. *Journal of Applied Ecology*, 50, 1341–1349. <https://doi.org/10.1111/1365-2664.12155>
- Duarte, C. M., Agusti, S., Barbier, E., Britten, G. L., Castilla, J. C., Gattuso, J. P., Fulweiler, R. W., Hughes, T. P., Knowlton, N., Lovelock, C. E., Lotze, H. K., Predragovic, M., Poloczanska, E., Roberts, C., & Worm, B. (2020). Rebuilding marine life. *Nature*, 580(7801), 39–51. <https://doi.org/10.1038/s41586-020-2146-7>
- Effrosynidis, D., Arampatzis, A., & Sylaios, G. (2018). Seagrass detection in the Mediterranean: A supervised learning approach. *Ecological Informatics*, 48, 158–170. <https://doi.org/10.1016/j.ecoinf.2018.09.007>
- Eisavi, V., Homayouni, S., Yazdi, A. M., & Alimohammadi, A. (2015). Land cover mapping based on random forest classification of multitemporal spectral and thermal images. *Environmental Monitoring and Assessment*, 187(5), 1–14. <https://doi.org/10.1007/s10661-015-4489-3>
- Fauzan, M. A., Kumara, I. S. W., Yogyantoro, R., Suwardana, S., Fadhillah, N., Nurmalarasi, I., Apriyani, S., & Wicaksono, P. (2017). Assessing the Capability of Sentinel-2A Data for Mapping Seagrass Percent Cover in Jerowaru, East Lombok. *Indonesian Journal of Geography*, 49(2), 195–203.
- Fauzan, M. A., Wicaksono, P., & Hartono. (2021). Characterizing Derawan seagrass cover change with time-series Sentinel-2 images. *Regional Studies in Marine Science*, 48, 102048. <https://doi.org/10.1016/j.rsma.2021.102048>
- Fourqurean, J. W., Duarte, C. M., Kennedy, H., Marbà, N., Holmer, M., Mateo, M. A., Apostolaki, E. T., Kendrick, G. A., Krause-Jensen, D., McGlathery, K. J., & Serrano, O. (2012). Seagrass ecosystems as a globally significant carbon stock. *Nature Geoscience*, 5, 505–509.
- Genuer, R., & Poggi, J.-M. (2020). *Random Forests with R*. In Use R!. Springer. <https://doi.org/10.1007/978-3-030-56485-8>
- Grech, A., Chartrand-Miller, K., Erftemeijer, P., Fonseca, M., McKenzie, L., Rasheed, M., Taylor, H., & Coles, R. (2012). A comparison of threats, vulnerabilities and management approaches in global seagrass bioregions. *Environmental Research Letters*, 7(2). <https://doi.org/10.1088/1748-9326/7/2/024006>
- Green, E. P., Mumby, P. J., Edwards, A. J., & Clark, C. D. (2000). *Remote Sensing Handbook for Tropical Coastal Management*. In Coastal Management Sourcebooks 3 (Issue January 2000).Ginting, D. N. B., Wicaksono, P., & Farda, N. M. (2023). Mapping Benthic Habitat From Worldview-3 Image Using Random Forest Case Study: Nusa Lembongan, Bali, Indonesia. *International Archives of the Photogrammetry, Remote Sensing and Spatial Information Sciences - ISPRS Archives*, 48(4/W6-2022), 123–129. <https://doi.org/10.5194/isprs-archives-XLVIII-4-W6-2022-123-2023>
- Hedley, J. D., Harborne, A. R., & Mumby, P. J. (2005). Simple and robust removal of sun glint for mapping shallow-water benthos. *International Journal of Remote Sensing*, 26(10), 2107–2112. <https://doi.org/10.1080/01431160500034086>
- Hedley, J. D., Roelfsema, C. M., Chollett, I., Harborne, A. R., Heron, S. F., Weeks, S. J., Skirving, W. J., Strong, A. E., Mark, E. C., Christensen, T. R. L., Ticzon, V., Bejarano, S., & Mumby, P. J. (2016). Remote sensing of coral reefs for monitoring and management: A review. *Remote Sensing*, 8(2). <https://doi.org/10.3390/rs8020118>
- Hochberg, E. J., Andréfouët, S., & Tyler, M. R. (2003). Sea surface correction of high spatial resolution ikonos images to improve bottom mapping in near-shore environments. *IEEE Transactions on Geoscience and Remote Sensing*, 41(7 PART II), 1724–1729. <https://doi.org/10.1109/TGRS.2003.815408>
- Holon, F., Boissery, P., Guilbert, A., Freschet, E., & Deter, J. (2015). The impact of 85 years of coastal development on shallow seagrass beds (*Posidonia oceanica* L. (Delile)) in South Eastern France: A slow but steady loss without recovery. *Estuarine, Coastal and Shelf Science*, 165(May), 204–212. <https://doi.org/10.1016/j.ecss.2015.05.017>
- Kabupaten Klungkung. (2012). Rencana Pengelolaan KKP Nusa Penida. Kabupaten Klungkung, Provinsi Bali.
- Khogkhao, C., Hayashizaki, K. I., Tuntiprapas, P., & Pratthep, A. (2017). Changes in seagrass communities along the runoff gradient of the Trang river, Thailand. *ScienceAsia*, 43(6), 339–346. <https://doi.org/10.2306/scienceasia1513-1874.2017.43.339>
- Koedsin, W., Intararuang, W., Ritchie, R. J., & Huete, A. (2016). An integrated field and remote sensing method for mapping seagrass species, cover, and biomass in Southern Thailand. *Remote Sensing*, 8(4). <https://doi.org/10.3390/rs8040292>
- Kovacs, E., Roelfsema, C., Lyons, M., Zhao, S., Phinn, S. Seagrass habitat mapping: How do landsat 8 OLI, sentinel-2, ZY-3A, and worldview-3 perform? *Remote Sens Lett* [Internet]. 2018;9(7):686–95. Available from: <https://doi.org/10.1080/2150704X.2018.1468101>
- Kumara, I. S. W. (2018). Pemetaan spesies lamun melalui integrasi citra multispektral dan pola respon spektral di Nusa Lembongan, Bali. (Skripsi yang tidak dipublikasikan). Universitas Gadjah Mada, Indonesia.
- Lillesand, T. M., Kiefer, R. F., & Chipman, J. W. (2015). *Remote Sensing and Image Interpretation* (7th ed.). Photogrammetric Engineering and Remote Sensing, 81(8). <https://doi.org/10.14358/pers.81.8.615>
- Lyons, M., Roelfsema, C., Kovacs, E., Samper-Villarreal, J., Saunders, M., Maxwell, P., & Phinn, S. (2015). Rapid monitoring of seagrass biomass using a simple linear modelling approach, in the field and from space. *Marine Ecology Progress Series*, 530, 1–14. <https://doi.org/10.3354/meps11321>
- Macreadie, P. I., Serrano, O., Maher, D. T., Duarte, C. M., & Beardall, J. (2017). Addressing calcium carbonate cycling in blue carbon accounting. *Limnology And Oceanography Letters*, 2(6), 195–201. <https://doi.org/10.1002/lol2.10052>

- Lyzenga, D. R. (1978). Passive remote sensing techniques for mapping water depth and bottom features. *Applied Optics*, 17(3), 379. <https://doi.org/10.1364/ao.17.000379>
- Macreadie, P. I., Anton, A., Raven, J. A., Beaumont, N., Connolly, R. M., Friess, D. A., Kelleway, J. J., Kennedy, H., Kuwae, T., Lavery, P. S., Lovelock, C. E., Smale, D. A., Apostolaki, E. T., Atwood, T. B., Baldock, J., Bianchi, T. S., Chmura, G. L., Eyre, B. D., ... Duarte, C. M. (2019). The Future of Blue Carbon Science. *Nature Communications*, 10(1), 1–13. <https://doi.org/10.1038/s41467-019-11693-w>
- Maxwell, A. E., Warner, T. A., & Fang, F. (2018). Implementation of machine-learning classification in remote sensing: An applied review. *International Journal of Remote Sensing*. Taylor and Francis Ltd. <https://doi.org/10.1080/01431161.2018.1433343>
- McLeod, E., Chmura, G. L., Bouillon, S., Salm, R., Bjork, M., Duarte, C. M., Lovelock, C. E., Schlesinger, W. H., & Silliman, B. R. (2011). A Blueprint For Blue Carbon: Toward An Improved Understanding Of The Role Of Vegetated Coastal Habitats in Sequestering CO₂. *Frontiers in Ecology and the Environment*, 9, 552–260.
- Munir, M., & Wicaksono, P. (2019). Support vector machine for seagrass percent cover mapping using PlanetScope image in Labuan Bajo, East Nusa Tenggara. December, 112. <https://doi.org/10.1117/12.2541849>
- Negara, I. K. S., Astawa Karang, I. W. G., & Giri, P. I. N. (2020). Simpanan karbon padang lamun di Kawasan Pantai Nusa Lembongan, Klungkung, Bali. *Journal of Marine Research and Technology*, 3(2), 82. <https://doi.org/10.24843/jmrt.2020.v03.i02.p04>
- Ozer, D. J. (1985). Correlation and the coefficient of determination. *Psychological Bulletin*, 97(2), 307–315. <https://doi.org/10.1037/0033-2909.97.2.307>
- Pham, T., Xia, J., Thang Ha, N., Tien Bui, D., Nhu Le, N., & Tekeuchi, W. (2019). A review of remote sensing approaches for monitoring blue carbon ecosystems: Mangroves, sea grasses and salt marshes during 2010–2018. *Sensors (Switzerland)*, 19(8). <https://doi.org/10.3390/s19081933>
- Prasetya, D., Supriharyono, M., Anggoro, S., & Sya'Rani, L. (2017). Coral bleaching on Lembongan Island, Nusa Penida, Bali. 134 (Iciran), 66–72. <https://doi.org/10.2991/iciran-17.2017.13>
- Roelfsema, C. M., Lyons, M., Kovacs, E. M., Maxwell, P., Saunders, M. I., Samper-Villarreal, J., & Phinn, S. R. (2014). Multi-temporal mapping of seagrass cover, species and biomass: A semi-automated object based image analysis approach. *Remote Sensing of Environment*, 150, 172–187. <https://doi.org/10.1016/j.rse.2014.05.001>
- Salford Systems. (2014). *Random Forests for Beginners*. Salford Systems, 71.
- Seagrass Watch. Percent Cover Standards. Online at <https://www.seagrasswatch.org/manuals/>, accessed April 10, 2022
- Sjafrie, N. D. M., Hernawan, U. E., Prayudha, B., Supriyadi, I. H., Iswari, M. Y., Rahmat, & Anggaraini, K. (2018). Status Padang Lamun Indonesia. P2OLIPi.
- Smith, G. (2018). Step away from stepwise. *Journal of Big Data*, 5(1). <https://doi.org/10.1186/s40537-018-0143-6>
- Strydom, M., Veldtman, R., Ngwenya, M. Z., & Esler, K. J. (2017). Invasive Australian Acacia seed banks: Size and relationship with stem diameter in the presence of gall-forming biological control agents. *PLoS ONE*, 12(8), 1–16. <https://doi.org/10.1371/journal.pone.0181763>
- Tamondong, A. M., Blanco, A. C., Fortes, M. D., & Nadaoka, K. (2013). Mapping of seagrass and other benthic habitats in Bolinao, Pangasinan using Worldview-2 satellite image. In *Proceedings of the IGARSS 2013—2013 IEEE International Geoscience and Remote Sensing Symposium*, Melbourne, VIC, Australia, 21–26 July 2013; Pp. 1579–1582. <https://doi.org/10.1109/IGARSS.2013.6723091>
- Ting, K. M. (2017). Confusion Matrix. In *Encyclopedia of Machine Learning and Data Mining*. Encyclopedia of Machine Learning and Data Mining. <https://doi.org/10.1007/978-1-4899-7687-1>
- Thompson, B. (1995). Stepwise regression and stepwise discriminant analysis need not apply here: A guidelines editorial (Educational Researcher, pp. 525–534). Sage Publications, Inc.
- UNEP. (2020). Out of Blue: The value of seagrasses to the environment and to people.
- Wahyudi, A. J., Rahmawati, S., Irawan, A., Hadiyanto, H., Prayudha, B., Hafizt, M., Afdal, A., Adi, N. S., Rustam, A., Hernawan, U. E., Rahayu, Y. P., Iswari, M. Y., Supriyadi, I. H., Solihudin, T., Ati, R. N. A., Kepel, T. L., Kusumaningtyas, M. A., Daulat, A., Salim, H. L., ... Kiswara, W. (2020). Assessing Carbon Stock and Sequestration of the Tropical Seagrass Meadows in Indonesia. *Ocean Science Journal*, 55(1), 85–97. <https://doi.org/10.1007/s12601-020-0003-0>
- Wang, G., & Jain, W. (2003). *Regression Analysis Modeling dan Forecasting*. Graceway Publishing Company.
- Wicaksono, P., Danoedoro, P., Hartono, Nehren, U., Maishella, A., Hafizt, M., Arjasakusuma, S., & Harahap, S. D. (2021). Analysis of field seagrass percent cover and aboveground carbon stock data for non-destructive aboveground seagrass carbon stock mapping using worldview-2 image. *International Archives of the Photogrammetry, Remote Sensing and Spatial Information Sciences - ISPRS Archives*, 46(4/W6-2021), 321–327. <https://doi.org/10.5194/isprs-Archives-XLVI-4-W6-2021-321-2021>
- Wicaksono, P., Lazuardi, W., & Munir, M. (2019). Integrating image at different spatial resolutions and field data for seagrass percent cover mapping. *International Archives of the Photogrammetry, Remote Sensing and Spatial Information Sciences - ISPRS Archives*, 42(4/W19), 487–492. <https://doi.org/10.5194/isprs-archives-XLII-4-W19-487-2019>
- Wicaksono, P. (2015). Remote sensing model development for seagrass and mangroves carbon stock mapping. (Unpublished doctoral dissertation). Universitas Gadjah Mada, Indonesia.
- Wicaksono, P., & Lazuardi, W. (2019). Random forest classification scenarios for benthic habitat mapping using planetscope image. *International Geoscience and Remote Sensing Symposium (IGARSS)*, 346, 8245–8248. <https://doi.org/10.1109/IGARSS.2019.8899825>
- Yaakub, S. M., McKenzie, L. J., Erftemeijer, P. L. A., Bouma, T., & Todd, P. A. (2014). Courage under fire: Seagrass persistence adjacent to a highly urbanised city-state. *Marine Pollution Bulletin*, 83(2), 417–424. <https://doi.org/10.1016/j.marpolbul.2014.01.012>
- Zhang, C., & Xie, Z. (2012). Combining object-based texture measures with a neural network for vegetation mapping in the Everglades from hyperspectral imagery. *Remote Sensing of Environment*, 124, 310–320. <https://doi.org/10.1016/j.rse.2012.05.021>
- Zhang, C., Selch, D., Xie, Z., Roberts, C., Cooper, H., & Chen, G. (2013). Object-based benthic habitat mapping in the Florida Keys from hyperspectral imagery. *Estuarine, Coastal and Shelf Science*, 134, 88–97. <https://doi.org/10.1016/j.ecss.2013.07.017>
- Zoffoli, M. L., Frouin, R., & Kampel, M. (2014). Water column correction for coral reef studies by remote sensing. *Sensors*, 14(9), 16881–16901. <https://doi.org/10.3390/s140916881>